

The sensitivity of Photosystem II to damage by UV-B radiation depends on the oxidation state of the water-splitting complex

András Szilárd, László Sass, Zsuzsanna Deák, Imre Vass *

Institute of Plant Biology, Biological Research Center of the Hungarian Academy of Sciences, P.O. Box 521, H-6701 Szeged, Hungary

Received 29 September 2006; received in revised form 15 November 2006; accepted 21 November 2006

Available online 15 December 2006

Abstract

The water-oxidizing complex of Photosystem II is an important target of ultraviolet-B (280–320 nm) radiation, but the mechanistic background of the UV-B induced damage is not well understood. Here we studied the UV-B sensitivity of Photosystem II in different oxidation states, called S-states of the water-oxidizing complex. Photosystem II centers of isolated spinach thylakoids were synchronized to different distributions of the S₀, S₁, S₂ and S₃ states by using packages of visible light flashes and were exposed to UV-B flashes from an excimer laser ($\lambda = 308$ nm). The loss of oxygen evolving activity showed that the extent of UV-B damage is S-state-dependent. Analysis of the data obtained from different synchronizing flash protocols indicated that the UV-sensitivity of Photosystem II is significantly higher in the S₃ and S₂ states than in the S₁ and S₀ states. The data are discussed in terms of a model where UV-B-induced inhibition of water oxidation is caused either by direct absorption within the catalytic manganese cluster or by damaging intermediates of the water oxidation process.

© 2006 Elsevier B.V. All rights reserved.

Keywords: UV-damage; Photosystem II; Oxygen evolution; S-states

1. Introduction

Ultraviolet-B (UV-B, 280–320 nm) radiation is a harmful component of sunlight that damages all forms of biological organisms [1,2]. In case of plants a well-recognized effect is a direct inhibition of photosynthesis [3,4]. Within the photosynthetic apparatus the most UV-B sensitive component is the light energy converting Photosystem II complex, whose electron transport capacity is inhibited and protein structure is damaged (for reviews see Refs. [3,5]). PSII is a water/plastoquinone oxido/reductase embedded in the thylakoid membrane, which transfers the electrons liberated from light-induced oxidation of water to membrane soluble plastoquinone molecules (for reviews see Refs. [6–8]). The side-product of PSII function is molecular oxygen, which has been the source of atmospheric oxygen during the course of evolution, and hence is the origin of the UV-B screening ozone veil that protects life on Earth.

The redox cofactors of PSII electron transport are bound to or contained by the D1 and D2 protein subunits, which form the reaction center of PSII [9]. Primary charge separation between the reaction center chlorophyll (P₆₈₀) and pheophytin is followed by rapid charge stabilization processes. On the acceptor side of PSII the electron from reduced pheophytin is transferred to the first, Q_A, and then to the second, Q_B, plastoquinone electron acceptor. On the donor side, P₆₈₀⁺ is reduced by Tyr-Z, a redox active tyrosine of the D1 protein, which then extracts an electron from the water-oxidizing complex (see Ref. [8]). Water oxidation is catalyzed by a cluster of four Mn ions which undergo light-induced changes in their oxidation states, called S-states. The complex cycles through five S-states denoted as S₀, ..., S₄ and oxygen is released during the S₃ → S₄ → S₀ transition, in which S₄ is a short-lived intermediate (for reviews see Refs. [7,10–12]).

The mechanism of damage induced by UV-B light to the electron transport and protein structure of PSII has been addressed by a number of studies both *in vitro* and *in vivo*. According to a widely accepted view, UV-B damages mainly the donor side of PSII by inactivating the Mn cluster of water oxidation [13–17], and with a smaller efficiency, the Tyr-D and

Abbreviations: PSII, Photosystem II; PQ, plastoquinone; DCMU

* Corresponding author. Tel.: +36 62 599 700; fax: +36 62 433 434.

E-mail address: imre@brc.hu (I. Vass).

Tyr-Z donors [14–16,18]. However, UV-B-induced modification or loss in the function of the Q_A and Q_B quinone electron acceptors [13,16,17,19,20] have also been observed.

Although UV-B-induced damage of the catalytic Mn cluster, resulting in the inhibition of electron transfer to Tyr-Z⁺ and P680⁺, and of the reaction center protein is well documented, the mechanistic background of this inhibitory effect has not been clarified. UV-B quanta are expected to exert their damaging effect in the vicinity of the target site where they are absorbed. It has been shown by several groups that the S-state transitions are accompanied by absorption changes which increase the overall UV-B absorption cross section of the catalytic Mn cluster with the progress of the S-state cycle [21–23]. In addition, the water-oxidation process may involve peroxidic intermediates [10,11,24], which are potential targets of UV-induced photolysis leading to the formation of highly reactive free radicals [25]. Consequently, the damaging efficiency of UV-B radiation may depend on the oxidation state of the catalytic Mn cluster, whose understanding could provide deeper insight into the mechanism of UV-B induced inactivation.

Here we used monochromatic UV-B laser flashes to study the UV-B sensitivity of PSII synchronized to different oxidation states of the water-oxidizing complex. Our data show that UV-B induced damage of oxygen evolution is S-state dependent, exhibiting higher sensitivity in the higher (S_3 , S_2) than in the lower (S_1 , S_0) S-states, which is likely to be related to UV-B absorption either directly by the Mn cluster or by intermediates of the water oxidizing process.

2. Materials and methods

2.1. Sample preparation

Thylakoid membranes were isolated from spinach with standard methods and were stored at -80°C until use in 0.4 M sucrose, 5 mM MgCl_2 , 10 mM NaCl and 40 mM HEPES (pH 7.5) at $2\text{--}3\text{ mg mL}^{-1}$.

2.2. UV-B treatment

UV-B flashes were provided by a Lambda Physics excimer laser ($\lambda=308\text{ nm}$) with 20 ns pulse width and 50 mJ energy per pulse. For synchronization of the S-states a Xenon flash lamp (General Radio, Stroboslave 3 μs , 0.5 J) was used. Any short wavelength UV radiation ($\lambda<330\text{ nm}$) from the Xenon flash was screened out by a plastic filter. Illumination of the samples was performed in a 1-cm quartz cuvette at room temperature at $30\text{ }\mu\text{g Chl mL}^{-1}$ under continuous stirring. In the applied arrangement the Xenon flash illuminated the whole 3 mL volume of the thylakoid suspension in the cuvette, but the laser flash hit only 1 mL volume, which was taken into correction for the calculation of S-state distributions. The illumination protocol contained packages of three synchronizing Xenon flashes fired at 1 Hz frequency and one UV-B laser flash given either before the Xenon flashes or after the 1st, 2nd, or 3rd Xenon flash (Table 1). The flash packages were separated by 100 s dark intervals to ensure the relaxation of the higher S-states. For a comparative measurement, UV-B damage was also induced by illumination from a broad-band UV-B source, (Vilbert Lournat VL-215 M), which emits in the 290–370 nm range with maximum at 312 nm [26]. The UV-B intensity was 2.66 W m^{-2} as measured by a Cole-Parmer radiometer (97503-30) equipped with a 312 nm sensor.

In order to calculate the S-state distributions following different flash protocols a modified version of the Joliot–Kok model was used, which takes into account the decay of higher S-states during the dark period between the

Table 1

Distribution of the S-states after various flash protocols

Flash protocol	S-state distribution (%)				Dominating S-state
	S_0	S_1	S_2	S_3	
UV, Xe, Xe, Xe	37.4	54.6	5.0	3.0	S_1
Xe, UV, Xe, Xe	8.2	39.0	46.6	6.2	S_2
Xe, Xe, UV, Xe	7.7	12.8	39.2	40.3	S_3
Xe, Xe, Xe, UV	35.4	9.4	16.6	38.6	S_0

The data are calculated with the assumptions that the initial distribution of the S-states in the dark is 25, 75, 0, 0% for S_0 , S_1 , S_2 , S_3 , respectively. The probability of misses and double hits is 0.15 and 0.03. The effect of the UV laser flash (UV) is taken into account by assuming that it hits only one third of the sample volume, but in this volume it induces the same S-state advancements as the Xenon flash. The Xenon flashes are fired at 1-s intervals and followed by the UV laser flash with 100-ms delay. The whole flash protocol consisted of 80 flash packages shown in the 1st column, separated by 100 s dark intervals. Due to the decay of the S_2 and S_3 states during the dark intervals between the flash packages the S-state distributions change at the beginning of the flash treatment (up to 5–10 flash packages), but reach equilibrium level afterwards. The data in the table show the equilibrium values, which are reached before the UV flash was fired. The last column indicates the name of the S-state that dominates the distribution during the given flash protocol.

flash packages [27]. For this model the initial distribution of the S_0 and S_1 states (25 and 75%, respectively), the miss (15%) and double hit (3%) parameters were obtained from flash-induced oxygen evolution measurement using a home-built flash-oxygen electrode as described earlier [28]. The room temperature decay half-lifetimes of the S_2 (25 s) and S_3 (35 s) were calculated from an earlier published work [28]. The validity of these decay times was confirmed by measuring the flash oxygen pattern after various dark intervals following one or two preflashes. For the calculation of S-state distributions it was also assumed that the UV-B laser flash induced S-state transitions in a same way as the Xenon flashes, which was experimentally verified by flash induced oxygen evolution measurements.

Steady-state rates of oxygen evolution were measured by using a Hansatech DW2 O_2 electrode at saturating $1000\text{ }\mu\text{Em}^{-2}\text{ s}^{-1}$ light intensity in the presence of 0.5 mM 2,5-dimethyl-P-benzoquinone as electron acceptor. Typically, 2 mL of cells at $10\text{ }\mu\text{g Chl a mL}^{-1}$ were used in each measurement.

3. Results

To design the experimental protocol for our study, first we had to consider the effect of synchronizing Xenon flashes on PSII activity. It has been shown previously that PSII can be photodamaged by short visible light flashes if they were separated by large enough intervals to allow charge recombination of the $S_2Q_B^-$ and $S_3Q_B^-$ charge pairs [29,30]. To clarify the damaging potential of the synchronizing Xenon flashes on PSII activity, the samples were illuminated by a similar protocol as used for the UV experiments, but this time without UV flashes, i.e. 80 packages of 1, 2, 3, or 4 flashes were fired with 1-s delay between the flashes and 100-s delay between the packages. As shown in Fig. 1, this illumination protocol induced S-state dependent inactivation of PSII activity, with maximum after the two flash containing packages, and minimum after the four flash containing packages. This effect is consistent with the model suggesting that the $S_2Q_B^-$ and $S_3Q_B^-$ recombinations damage the PSII centers [29,30]. To minimize the influence of the synchronizing Xenon flashes on the UV-induced inhibition of PSII activity we have chosen a flash protocol in which three Xenon flashes plus one UV-B flash was applied, and the

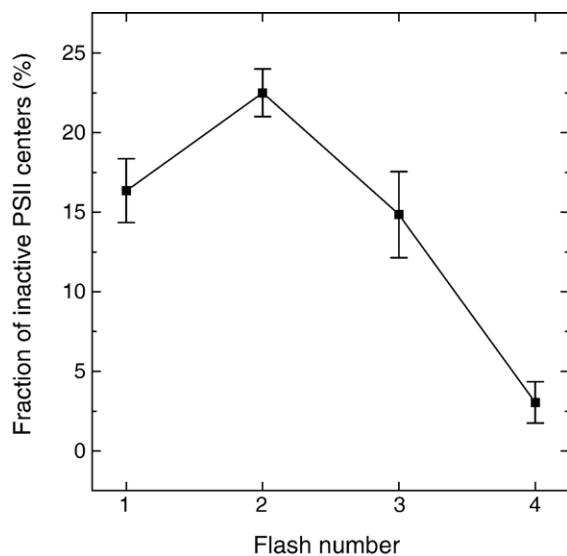


Fig. 1. The effect of synchronizing Xenon flashes on the oxygen evolving activity of PSII. Samples were illuminated with 80 flash packages separated by 100 s dark intervals, each of them containing 1, 2, 3 or 4 Xe flashes given at 1 Hz frequency. The fraction of inactive PSII centers was calculated from the decrease of oxygen evolving activity of the illuminated samples relative to the control, which was kept under the same conditions for the duration of the measurement, but in darkness. The data show the average of three independent experiments with the indicated standard error.

position of the UV-B flash was varied relative to the Xenon flashes (Table 1). By using this protocol the majority of the center always end up in the S_1 state leaving Q_B^- without recombination partner during the long (100 s) intervals between the flash packages.

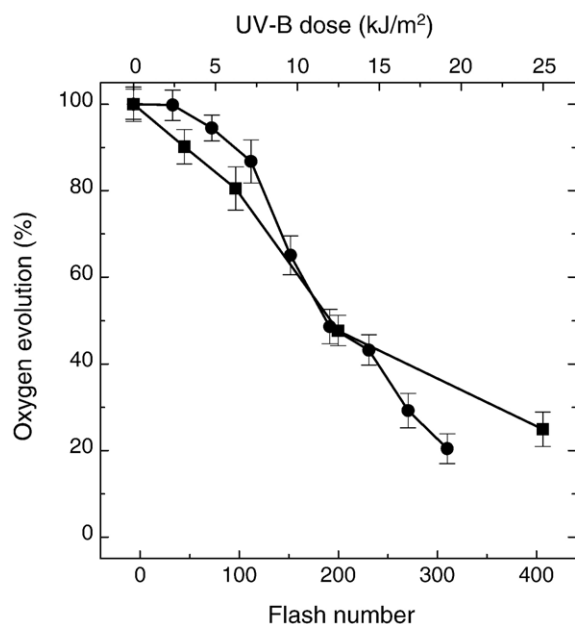


Fig. 2. Dose-effect curves of UV-B damage induced by short laser flashes and continuous illumination. Thylakoids were exposed to either a series of 308 nm laser flashes at 1 Hz frequency (squares) or to continuous illumination from a broad-band UV-B source (circles). The loss of oxygen evolving activity is plotted as a function of flash number and cumulative UV-B dose.

Fig. 2 shows the extent of PSII inactivation induced by different number of UV-B flashes. In order to optimize conditions for well detectable PSII damage and reasonable length of the treatment, considering the 100 s intervals between the synchronizing packages, we have chosen to use 80 UV-B flashes for the inactivation experiments, which correspond to 4.5 kJ m^{-2} cumulative dose. Fig. 2 shows also the dose dependence of PSII inactivation when induced by a broad-band continuous UV-B source. The dose-effect curves are following a largely parallel course. The apparently smaller damaging effect of the continuous irradiation at the same dose most likely arises from the broad spectral distribution of the UV-B lamp ranging from 290 to 370 nm, in which the less damaging longer wavelength components have a substantial weight, in contrast to the monochromatic 308 nm emission of the excimer laser.

The effect of UV-B treatments on PSII activity performed according to the flash protocols listed in Table 1 is shown in Fig. 3. The fraction of PSII centers, which were damaged by UV-B light were calculated from the loss of oxygen evolution in the irradiated samples relative to the control ones kept under the same conditions, but in darkness (Fig. 3). The figure also shows the S state whose concentration is dominating after each flash

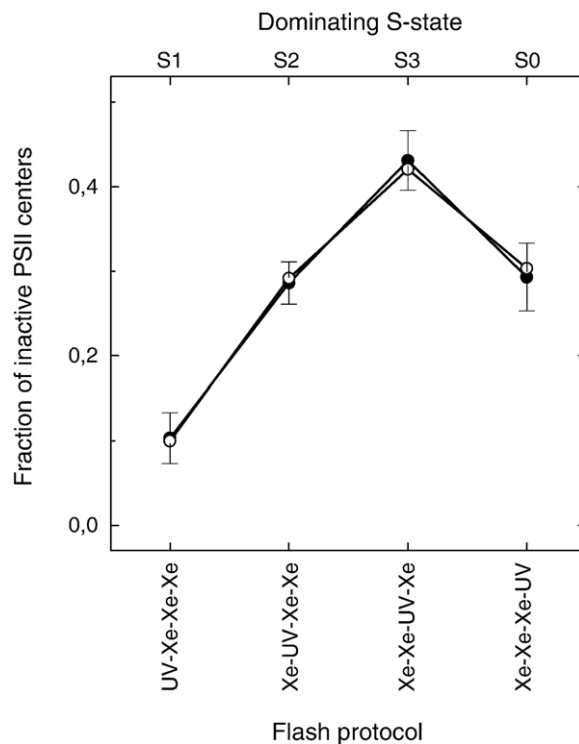


Fig. 3. The S-state dependence of UV-B induced damage of oxygen evolution from Photosystem II. Thylakoids were exposed to various illumination protocols (listed in Table 1), which ensure that the damaging UV-B laser flashes hit the PSII centers in different S-state distributions whose dominating species is indicated on the x axis. The fraction of damaged PSII centers (full symbols) was calculated from the loss of oxygen evolving activity after 80 flash packages relative to control thylakoids, which were kept under the same conditions for the duration of the measurements, but in the dark. The empty symbols show the result of best fit of principal component analysis, which was used to calculate the damaging weight of UV-B in the different S-states. In this analysis the averaged data from three different experiments were used.

protocol. It can be seen that the UV-B induced damage is substantially higher in the S_3 and S_2 than in the S_1 and S_0 states. Since in all flash protocols a considerable amount of centers was in other S-states than the dominating one (Table 1), Fig. 3 can give only a rough estimation of the S-state dependence of UV-B sensitivity. In order to obtain more precise information, the data were subjected to a principal component analysis. Here the fraction of inactivated centers is expressed as

$$I_i = P_0 S_{0,i} + P_1 S_{1,i} + P_2 S_{2,i} + P_3 S_{3,i},$$

where P_0, \dots, P_3 represent the sensitivity of PSII in the S_0, \dots, S_3 states, respectively. $S_{0,i}, \dots, S_{3,i}$ are the S-state distributions which correspond to a particular flash protocol. Whereas, I_i is the fraction of inhibited PSII centers induced by the i th flash protocol. By using the measured fractions of inactivated centers as well as the calculated S-state distributions as input data the sensitivity factors were determined by a least-squares minimization procedure. Since the sensitivity factors represent the damaging weight of 80 UV-B flashes, they were normalized to the highest value to obtain data, which reflect the relative sensitivity of PSII in the different S-states. According to the results shown in Fig. 4A, the relative sensitivity of PSII to UV-B induced damage is very small in the S_0 state, somewhat larger in S_1 , and high in the S_3 and S_2 states.

4. Discussion

The sensitivity of the water-oxidizing complex to damage by UV-B radiation is well documented both in isolated and intact systems [13–17]. However, the mechanism of damage has not been clarified. The data available so far indicate an all or nothing type inhibition of PSII by UV-B. This is shown by the unchanged oscillatory pattern of flash-induced oxygen evolution [31], 830 nm absorbance change [15], and thermoluminescence intensity [14]. Consequently, UV-B radiation does not modify the S-state distribution and transition probabilities in the still active centers and does not cause a specific block at one or more S-state transitions. The loss of the multiline EPR signal from the S_2 state and the lack of any EPR signal that could be assigned to a modified S_2 state also shows that after hit by UV-B the water-oxidizing complex becomes completely inactive [16]. It is also unlikely that UV-B would cause the release of the Ca^{2+} or Cl^- cofactors of oxygen evolution or of the Mn stabilizing 33 kDa peripheral protein. These effects induce clear signatures in thermoluminescence characteristics, such as temperature shift and modified oscillation of the main bands (see Ref. [32]), which have not been observed after UV-B induced damage [14]. Taken together, these data indicate that the damaging effect of UV-B should be located within the catalytic site and should cause a structural and/or functional change that renders the whole complex inactive.

Our results demonstrate that the oxygen evolving capacity of PSII shows S-state dependent sensitivity to UV-B radiation. Since the inactivation was induced by short, high energy laser flashes one has to consider possible artifacts which may arise from local heating of the sample. The Mn cluster of the water-

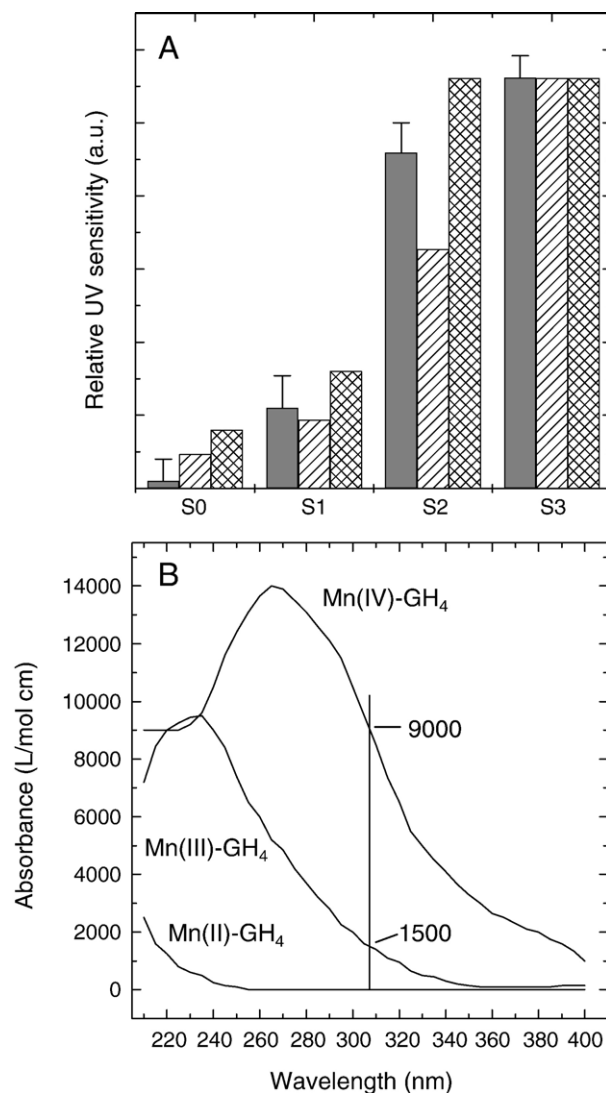


Fig. 4. (A) Relative UV-B sensitivity of the different S-states. The data obtained for the S-state dependent damage of oxygen evolution in Fig. 3 were analyzed by principal component analysis. The damaging weights calculated for the individual S-states are shown after normalization to the highest value obtained for S_3 (gray columns). These relative sensitivity values are compared with the results of calculations based on the assumption that UV sensitivity is related to Mn absorption changes of two Mn ions, which are sequentially oxidized from $\text{Mn(II)Mn(III)} \rightarrow \text{Mn(III)Mn(III)} \rightarrow \text{Mn(III)Mn(IV)} \rightarrow \text{Mn(IV)Mn(IV)}$ during the $S_0 \rightarrow S_1 \rightarrow S_2 \rightarrow S_3$ transitions, respectively, using the relative absorbance at 308 nm of Mn(II), Mn(III) and Mn(IV) containing organic complexes shown in part B (right hatched columns). The calculations were also made by using the assumption that no Mn oxidation occurs during the $S_2 \rightarrow S_3$ transition (cross hatched columns) (B) Absorption spectra of organic Mn–gluconate complexes containing Mn(II), Mn(III), or Mn(IV) based on Ref. [39]. The vertical line indicates the relative absorbance at the wavelength of the applied UV flash.

oxidizing complex is sensitive to high temperatures (see [33]), thus local heating could in principle cause inactivation of oxygen evolution. However, we are convinced that this effect can be neglected for the following reasons: (i) the dose–effect curve of UV-B inactivation by the laser flashes and by continuous illumination proceed via similar courses (Fig. 2). The somewhat smaller damage induced by the continuous UV-B source can be explained by the substantial contribution from

less damaging, longer wavelength emission from the lamp. (ii) Heat inactivation of PSII is known to induce a substantial increase in the so called F_0 chlorophyll fluorescence level (see [33]) which was not observed after the UV-B flashes (not shown). (iii) Heat induced inactivation of Mn cluster is not known to be an S-state dependent phenomenon.

Our finding that the UV-B sensitivity of the water-oxidizing complex is substantially higher in the S_3 and S_2 than in the S_1 and S_0 states should be related to differential UV susceptibility of the catalytic site in different stages of the water oxidation process. Although no consensus has yet emerged regarding the exact mechanism of water splitting, most of the available data agree on that the S-state transitions are accompanied by absorption changes in the UV-B range [22,23,34], which result in gradually increasing UV absorption cross section as the S-state cycle advances. The absorption increase which accompanies the $S_1 \rightarrow S_2$ transition has been assigned to an Mn (III) to Mn (IV) oxidation within the Mn cluster [22,23,34], which has been supported by EPR and X-ray spectroscopy (see [7,35]). The assignment of the absorption change during the $S_2 \rightarrow S_3$ transition is more controversial. Both Mn (III) to Mn (IV) oxidation [23,34] and the formation of an organic radical in the vicinity of the Mn cluster [22] have been proposed. EPR and X-ray spectroscopy also seem to support both Mn(III) to Mn(IV) oxidation [36,37], or the oxidation of a μ -oxo bridge [38] during the S_2 to S_3 transition. The relatively small absorption change during the $S_0 \rightarrow S_1$ transition was proposed to reflect Mn (II) to Mn (III) oxidation [34] or binding of Ca^{2+} to the Mn cluster [23]. Regardless of the precise assignment of the absorption changes that accompany the individual S-state transitions, it is obvious that the UV-B absorption cross section of the catalytic site of water oxidation gradually increases with the advancement of the S-states. If we assume that increased absorption of UV-B quanta within the Mn cluster and/or in its immediate vicinity can modify the structure of the catalytic site, the loss of oxygen evolving activity can be explained. This is in a good qualitative agreement with the pattern of UV-B sensitivity, which shows gradual increase from S_0 to S_3 with small steps between S_0 and S_1 , as well as S_2 and S_3 , and large increase between S_1 and S_2 . (Fig. 4A).

It has to be noted, however, that the Mn cluster contains two Mn (IV) ions also in the S_0 state (see [10,11,38]) which has very low sensitivity to UV-B. Thus, we have to refine the model by postulating that direct UV-B absorption is damaging only when it affects a subset of Mn ions within the cluster. Most models of water oxidation assumes that out of the four Mn ions only two is involved actively in water splitting, and only their oxidation state is changing during the S cycle (see [10,11,38]). The other two Mn ions are expected to keep their oxidation state in Mn (IV) throughout the whole S cycle. Thus, we propose that the damaging effect of UV-B absorption affects only the two Mn ions, which are actively involved in the water oxidation process. In that case the low UV-B sensitivity of the S_0 state could be explained by the Mn (II) and Mn (III) configuration of the active Mn ions.

The model, which relates increased UV sensitivity of the water oxidizing complex to Mn absorption as outlined above is further supported by absorption properties of organic Mn

complexes. Fig. 4B shows the absorption spectra of organic Mn–gluconate complexes, which contain either Mn(II), Mn(III) or Mn(IV) [39]. Their absorption coefficient is significantly higher in the Mn(IV), than in the Mn(III) and Mn(II) states. By approximating the relative UV absorption of the Mn(II), Mn (III), and Mn(IV) ions in the Mn cluster of water oxidation with those of the Mn–gluconate complexes we modeled the pattern of absorption changes of the Mn cluster in the different S states. These data are good qualitative agreement with the observed S-state dependence of UV sensitivity (Fig. 4B) supporting the importance of UV absorption within the Mn cluster in the inactivation of PSII.

The model outlined above describes qualitatively well the gradual increase of UV-B sensitivity during the S-state advancements. However, it does not provide deeper insight into the actual mechanism of damage. One obvious possibility to consider is that UV-B damages the structure of the Mn cluster by affecting one or more of its ligands. There is an interesting example in the literature for such effect, which shows that 355 nm UV flashes break up the structure of a synthetic Mn_4O complex in which the four Mn ions are connected by μ -oxo bridges and stabilized by 6 diphenylphosphinate anions on the outer surfaces of the cubane Mn_4O_4 structure [40]. In this complex the Mn ions are in the 2Mn(III) 2Mn(IV) mixed valence oxidation state and can be considered as a model of higher S-states. The UV pulse shoots out one of the stabilizing Ph_2PO_2^- ligands, which results in the break up of the symmetric Mn_4O_4 cluster and release of an O_2 molecule [40]. It is important to note that a laser pulse of similar intensity at 532 nm did not destroy the complex [40], i.e. the energy of UV photons is required for the inactivation. Even though the structure of the Mn cluster of water oxidation is different from that of the artificial complex, UV-induced destruction of a stabilizing ligand could be a mechanism by which water oxidation is inactivated.

Another approach to access the mechanism of UV-B induced damage of the catalytic site is to consider the effect of UV-B light on the intermediates of the water oxidation process. Some models of water oxidation assumes the production of peroxidic intermediates in the higher S-states prior to formation of S_4 [10,11,24,41]. Moreover, the presence of bound hydrogen peroxide at the donor side of PSII has also been suggested [42]. Hydrogen peroxide is known to be easily decomposed by ultraviolet light ($\lambda < 350$ nm), which results in highly damaging hydroxyl radicals [25]. Our earlier studies have demonstrated that the dominating reactive oxygen species induced by UV-B radiation in thylakoids is hydroxyl radicals [43]. Thus, UV-B induced photolysis of a peroxidic intermediate to highly damaging hydroxyl radicals in the heart of the Mn cluster would provide an attractive mechanism of UV-B induced damage. According to a model of Renger the peroxidic intermediate is formed in the S_3 state [8,10], which would be in good agreement with the highest UV-B sensitivity in this state, but cannot explain the smaller, but still significant UV-B sensitivity observed in the lower S-states. In the hydrogen atom abstraction model of water oxidation the two water molecules which bind to the catalytic site in the S_0 state undergo sequential deprotonation during the S-state cycle [11]. This results in the

formation of one Mn ligated OH group in the S₁ state, two in the S₂ state and one OH plus one O ligand in S₃ [11]. Assuming that the absorption of a UV-B photon can split the OH–Mn bond and form OH radical in the process, the gradually increasing UV-B sensitivity from S₀ to S₂ could be explained.

Other models of water oxidation favor the idea that the formation of the dioxygen bond occurs in a concerted reaction in the S₄ state without the involvement of partially oxidized intermediates (see Refs. [12,36]). In that case the increased UV-B absorption in the higher S-states could induce damage or modification of the protein environment around the Mn cluster and thereby disrupt the structure of the catalytic site.

Although the presently available data are not sufficient for an unambiguous mechanistic model of UV-B induced damage of the water oxidizing complex, we propose that is related to the function of the two Mn ions that actively participate in the water oxidation process. We prefer the idea that the damage is sensitized by S-state dependent UV-B absorption, which disrupts the structure of the Mn cluster and/or leads to the production of reactive oxygen species (hydroxyl radicals in particular) induced by interaction with peroxidic and/or hydroxyl ligand intermediates of water oxidation.

Acknowledgments

This work was supported by grants from European Union (MRTN-CT-2003-505069, and STREP-SOLAR-H-516510). Valuable help of András Dér with the UV laser flash experiments is appreciated.

References

- [1] J.B. Kerr, C.T. McElroy, Evidence for upward trends of ultraviolet-B radiation linked to ozone depletion, *Science* 262 (1993) 1032–1034.
- [2] R.C. Smith, B.B. Prézelin, K.S. Baker, R.R. Bidigare, N.P. Boucher, T. Coley, D. Karentz, S. MacIntyre, H.A. Matlick, D. Menzies, M. Ondrusek, Z. Wan, K.J. Waters, Ozone depletion: ultraviolet radiation and phytoplankton biology in Antarctic waters, *Science* 255 (1995) 952–959.
- [3] J.F. Bormann, Target sites of UV-B radiation in photosynthesis of higher plants, *J. Photochem. Photobiol., B* 4 (1989) 145–158.
- [4] M. Tevini, A.H. Teramura, UV-B effects on terrestrial plants, *Photochem. Photobiol.* 50 (1989) 479–487.
- [5] I. Vass, Adverse effects of UV-B light on the structure and function of the photosynthetic apparatus, in: M. Pessarakli (Ed.), *Handbook of Photosynthesis*, Marcel Dekker, Inc., New York, 1996, pp. 931–950.
- [6] B. Andersson, S. Styring, Photosystem II: molecular organization, function, and acclimation, *Curr. Top. Bioenerg.* 16 (1991) 1–81.
- [7] R.J. Debus, The manganese and calcium ions of photosynthetic oxygen evolution, *Biochim. Biophys. Acta* 1102 (1992) 269–352.
- [8] G. Renger, Photosynthetic water oxidation to molecular oxygen: apparatus and mechanism, *Biochim. Biophys. Acta* 1503 (2001) 210–228.
- [9] J. Barber, K. Ferreira, K. Maghlaoui, S. Iwata, Structural model of the oxygen-evolving centre of Photosystem II with mechanistic implications, *Phys. Chem. Chem. Phys.* 6 (2004) 4737–4742.
- [10] G. Renger, Mechanistic and structural aspects of photosynthetic water oxidation, *Physiol. Plant.* 100 (1997) 828–841.
- [11] C.W. Hoganson, G.T. Babcock, A metalloradical mechanism for the generation of oxygen from water in photosynthesis, *Science* 277 (1997) 1953–1956.
- [12] J. Messinger, Evaluation of different mechanistic proposals for water oxidation in photosynthesis on the basis of Mn₄O_xCa structures for the catalytic site and spectroscopic data, *Phys. Chem. Chem. Phys.* 6 (2004) 4764–4771.
- [13] G. Renger, M. Völker, H.J. Eckert, R. Fromme, S. Hohm-Veit, P. Graber, On the mechanism of Photosystem II deterioration by UV-B irradiation, *Photochem. Photobiol.* 49 (1989) 97–105.
- [14] É. Hideg, L. Sass, R. Barbato, I. Vass, Inactivation of oxygen evolution by UV-B irradiation. A thermoluminescence study, *Photosynth. Res.* 38 (1993) 455–462.
- [15] A. Post, P.B. Lukins, P.J. Walker, A.W.D. Larkum, The effects of ultraviolet irradiation on P₆₈₀⁺ reduction in PS II core complexes measured for individual S-states and during repetitive cycling of the oxygen-evolving complex, *Photosynth. Res.* 49 (1996) 21–27.
- [16] I. Vass, L. Sass, C. Spetea, A. Bakou, D. Ghanotakis, V. Petrouleas, UV-B induced inhibition of Photosystem II electron transport studied by EPR and chlorophyll fluorescence. Impairment of donor and acceptor side components, *Biochemistry* 35 (1996) 8964–8973.
- [17] I. Vass, D. Kirilovsky, A.-L. Etienne, UV-B radiation-induced donor- and acceptor-side modifications of Photosystem II in the cyanobacterium *Synechocystis* sp. PCC 6803, *Biochemistry* 38 (1999) 12786–12794.
- [18] C.T. Yerkes, D.M. Kramer, J.M. Fenton, A.R. Crofts, UV-photoinhibition: studies *in vitro* and in intact plants, in: M. Baltscheffsky (Ed.), *Current Research in Photosynthesis*, vol. II, Kluwer Academic Publisher, The Netherlands, 1990, pp. II.6.381–II.6.384.
- [19] A. Melis, J.A. Nemson, M.A. Harrison, Damage to functional components and partial degradation of Photosystem II reaction center proteins upon chloroplast exposure to ultraviolet-B radiation, *Biochim. Biophys. Acta* 1100 (1992) 312–320.
- [20] M.A.K. Jansen, B.M. Greenberg, M. Edelman, A.K. Mattoo, V. Gaba, Accelerated degradation of the D2 protein of Photosystem II under ultraviolet radiation, *Photochem. Photobiol.* 63 (1996) 814–817.
- [21] J.P. Dekker, H.J. van Gorkom, M. Brok, L. Ouwehand, Optical characterization of Photosystem II electron donors, *Biochim. Biophys. Acta* 764 (1984) 301–309.
- [22] J. Lavergne, Improved UV-visible spectra of the S-transitions in the photosynthetic oxygen-evolving system, *Biochim. Biophys. Acta* 1060 (1991) 175–188.
- [23] P.J. Leeuwen, C. Heimann, H.J. Gorkom, Absorbance difference spectra of the S-state transitions in Photosystem II core particles, *Photosynth. Res.* 38 (1993) 323–330.
- [24] J. Messinger, M. Badger, T. Wydrzynski, Detection of one slowly exchanging substrate water molecule in the S₃ state of Photosystem II, *Proc. Natl. Acad. Sci. U. S. A.* 92 (1995) 3209–3213.
- [25] G. Czapski, Reaction of OH, in: L. Pecker (Ed.), *Methods in Enzymology*, vol. 105, 1984, pp. 209–215.
- [26] Z. Máté, L. Sass, M. Szekeres, I. Vass, F. Nagy, UV-B induced differential transcription of *psbA* genes encoding the D1 protein of Photosystem II in the cyanobacterium *Synechocystis* 6803, *J. Biol. Chem.* 273 (1998) 17439–17444.
- [27] A. Szilárd, L. Sass, I. Vass, Photoinactivation of Photosystem II at low light intensity, *Mathematical models*, *Acta Biol. Szeged.* 46 (2002) 167–169.
- [28] I. Vass, Zs. Deák, É. Hideg, Charge equilibrium between the water-oxidizing complex and the donor tyrosine-D in Photosystem II, *Biochim. Biophys. Acta* 1017 (1990) 63–69.
- [29] N. Keren, A. Berg, P.J.M. van Kan, H. Levanon, I. Ohad, Mechanism of Photosystem II photoinactivation and D1 protein degradation at low light: the role of back electron flow, *Proc. Natl. Acad. Sci. U. S. A.* 94 (1997) 1579–1584.
- [30] A. Szilárd, L. Sass, É. Hideg, I. Vass, Photoinactivation of Photosystem II by flashing light, *Photosynth. Res.* 84 (2005) 15–20.
- [31] G. Renger, M. Voss, P. Graber, A. Schulze, Effect of UV radiation on different partial reactions of the primary processes of photosynthesis, in: C. Worrest, M.M. Caldwell (Eds.), *Stratospheric Ozone Reduction, Solar Ultraviolet Radiation and Plant Life*, Springer, Berlin, 1986, pp. 171–184.
- [32] I. Vass, Y. Inoue, Thermoluminescence in the Study of Photosystem Two, in: J. Barber (Ed.), *The Photosystems: Structure, Function and Molecular Biology*, Topics in Photosynthesis, vol. 11, Elsevier, Amsterdam, 1992, pp. 259–294.

- [33] E. Weis, J.A. Berry, Plants and high temperature stress, in: S.P. Long, F.I. Woodward (Eds.), *Plants and Temperature*, The Company of Biologists Limited, Cambridge, 1988, pp. 329–345.
- [34] H. Kretschmann, J.P. Dekker, Ö. Saygin, H.T. Witt, An agreement on the quaternary oscillation of ultraviolet absorption changes accompanying the water splitting in isolated Photosystem II complexes from the cyanobacterium *Synechococcus* sp. *Biochim. Biophys. Acta* 932 (1988) 358–361.
- [35] A.W. Rutherford, Photosystem II, the water-splitting enzyme, *Trends Biochem. Sci.* 14 (1989) 227–232.
- [36] M. Haumann, C. Müller, P. Liebisch, L. Iuzzolino, J. Dittmer, M. Grabolle, T. Neisius, W. Meyer-Klaucke, H. Dau, Structural and oxidation state changes of the Photosystem II manganese complex in four transitions of the water oxidation cycle ($S_0 \rightarrow S_1$, $S_1 \rightarrow S_2$, $S_2 \rightarrow S_3$, and $S_{3,4} \rightarrow S_0$) characterized by X-ray absorption spectroscopy at 20 K and room temperature, *Biochemistry* 44 (2005) 1894–1908.
- [37] T.A. Ono, T. Noguchi, Y. Inoue, M. Kusunoki, T. Matsushita, H. Oyanagi, X-ray detection of the period-four cycling of the manganese cluster in photosynthetic water oxidizing enzyme, *Science* 258 (1992) 1335–1337.
- [38] J. Messinger, J.H. Robblee, U. Bergmann, C. Fernandez, P. Glatzel, H. Visser, R.M. Cinco, K.L. McFarlane, E. Bellacchio, S.A. Pizarro, S.P. Cramer, K. Sauer, M.P. Klein, V.K. Yachandra, Absence of Mn-centered oxidation in the $S_2 \rightarrow S_3$ transition: implications for the mechanism of photosynthetic water oxidation, *J. Am. Chem. Soc.* 123 (2001) 7804–7820.
- [39] M.E. Bodini, L.A. Willis, T.L. Riechel, D.T. Sawyer, Electrochemical and spectroscopic studies of manganese(II), -(III), and -(IV) gluconate complexes: 1. Formulas and oxidation–reduction stoichiometry, *Inorg. Chem.* 15 (1976) 1538–1543.
- [40] W.F. Ruettinger, M. Yagi, K. Wolf, S. Bernasek, G.C. Dismukes, O_2 evolution from the manganese-oxo cubane core $Mn_4O_4^{6+}$: a molecular mimic of the photosynthetic water oxidation enzyme? *J. Am. Chem. Soc.* 122 (2000) 10353–10357.
- [41] L.I. Krishtalik, Energetics of multielectron reactions. Photosynthetic oxygen evolution, *Biochim. Biophys. Acta* 849 (1986) 162–171.
- [42] V.V. Klimov, G.M. Ananyev, O. Zastryzhnaya, T. Wydrzynski, G. Renger, Photoproduction of hydrogen peroxide in Photosystem II membrane fragments: a comparison of four signals, *Photosynth. Res.* 38 (1993) 409–416.
- [43] E. Hideg, I. Vass, UV-B induced free radical production in plant leaves and isolated thylakoid membranes, *Plant Sci.* 115 (1996) 251–260.